Available online at www.sciencedirect.com
SCIENCE DIRECT®
Journal of Sound and Vibration 283 (2005) 1–20
JOURNAL OF SOUND AND VIBRATION
www.elsevier.com/locate/jsvi

Input torque balancing using a cam-based centrifugal pendulum: design procedure and example

Bram Demeulenaere*, Pieter Spaepen, Joris De Schutter

Department of Mechanical Engineering, Katholieke Universiteit Leuven, Celestijnenlaan 300B, B-3001 Heverlee, Belgium

Received 23 June 2003; received in revised form 17 December 2003; accepted 4 March 2004
Available online 5 November 2004

Abstract

Input torque balancing is a well-known way to reduce drive speed fluctuations in high-speed machinery and combustion engines. This paper introduces a cam-based centrifugal pendulum (CBCP) and a design procedure for it which results in quasi-perfect balancing of inertial torques for any drive speed. The CBCP combines the centrifugal pendulum vibration absorber, well-known in mechanical vibration literature, with a torque balancing principle well-known in mechanism literature, that is, the use of cams to generate arbitrary torques. For given design parameters (such as the link lengths and link inertial parameters), the cam design is governed by a nonlinear, second-order, explicit differential equation. This differential equation is numerically solved by reformulating it as a nonlinear least-squares problem. The design parameters themselves are determined by means of an optimization problem, the goal of which is to minimize the (constant) equivalent inertia of the combined system, consisting of the original mechanism to be balanced and the CBCP. Application of the CBCP to torque balance a high-speed, purely inertial cam-follower mechanism, driving the sley of a weaving loom, shows that the optimization results in a compact and technologically feasible mechanism.

*Corresponding author. Tel.: +32-16-32-2551; fax: +32-16-32-2987. *Abbreviations*: ITB, input torque balancing; CPVA, centrifugal pendulum vibration absorber; TPVA, torsional pendulum vibration absorber; CBCP, cam-based centrifugal pendulum; TUVA, translational undamped dynamic vibration absorber; ODE, ordinary differential equation; rms, root mean square; rpm, revolutions per minute.

E-mail address: bram.demeulenaere@mech.kuleuven.ac.be (B. Demeulenaere).

0022-460X/$ - see front matter © 2005 Elsevier Ltd. All rights reserved.
doi:10.1016/j.jsv.2004.03.029

Nomenclature

t	time (s)
$(\dot{})$	first derivative w.r.t. time t
$(\ddot{})$	second derivative w.r.t. time t
T	period of motion (s)
ω	mean drive speed $= 2\pi/T$ (rad/s)
n	order of disturbing torque (dimensionless)
L_r	half of rotor length (m)
L_c	coupler (pendulum) length (m)
R_b	rolling body radius (m)
m_r, J_r	rotor mass (kg) and centroidal moment of inertia (kg m^2)
m_c, J_c	coupler mass (kg) and centroidal moment of inertia (kg m^2)
m_b, J_b	rolling body mass (kg) and centroidal moment of inertia (kg m^2)
X_c	location of the coupler center of mass along the line o_2–o_3 (m)
o_i	points defined in Fig. 1 ($i = \{1, 2, 2', 3, 3'\}$) and Fig. 2 ($i = \{4, 5\}$)
$h(t)$	rolling body rotation angle (rad)
$g(t)$	rotor rotation angle w.r.t. X-axis (rad)
$q(t)$	coupler rotation angle w.r.t. X-axis (rad)
$s(t)$	$\ddot{q}(t)\cos\left(\frac{2\pi}{T}t - q(t)\right) - \dot{q}\sin\left(\frac{2\pi}{T}t - q(t)\right)\left(\frac{2\pi}{T} - \dot{q}(t)\right)$
q_0	$q(t=0)$ (rad)
$M_c(t)$	CBCP input torque (N m)
$T_c(t)$	CBCP kinetic energy (J)
$M_o(t)$	original mechanism input torque (N m)
$T_o(t)$	original mechanism kinetic energy (J)
$E_o(t)$	original mechanism energy function (J)
$v_{Cc}(t)$	absolute velocity of the coupler center of mass (m/s)
$v_{Cb}(t)$	absolute velocity of the rolling body center of mass (m/s)
m^*	generalized mass (kg)
J_i^*	generalized moments of inertia (kg m^2) ($i = \{1, 2, 3\}$)
K	number of harmonics (dimensionless)
C	integration constant (rad)
a_k, b_k	unknown Fourier series amplitudes (rad)
$\mathbf{z}$	vector of unknown Fourier series amplitudes
$r_1(t, \mathbf{z})$	torque residual function (N m)
$r_2(t, \mathbf{z})$	energy residual function (J)
$\hat{q}_1$	approximate solution for q based on torque residual (rad)
$\hat{q}_2$	approximate solution for q based on energy residual (rad)
f_s	sample rate (Hz)
T_s	sample period (s)
J_{eq}	combined system equivalent inertia (kg m^2)
$J_{\text{eq},o}(t)$	original mechanism equivalent inertia (kg m^2)
$N_c(g)$	contact force between cam and rolling body (N)
$\sigma_H(g)$	Hertzian pressure in the cams (MPa)
$(\cdot)_{\max}$	$\max_{t\in[0,T]}(\cdot)$ or $\max_{g\in[0,2\pi]}(\cdot)$
$(\cdot)_{\min}$	$\min_{t\in[0,T]}(\cdot)$ or $\min_{g\in[0,2\pi]}(\cdot)$
$(\cdot)^M$	upper bound on $(\cdot)$
$(\cdot)^m$	lower bound on $(\cdot)$
L_b	lifetime of coupler-rolling body bearing (h)
L_c	lifetime of rotor-coupler bearing (h)
$f(t)$	cam–follower angular position (rad)
J	follower moment of inertia w.r.t. o_5 (kg m^2)
$r(g)$	radius of CBCP cam profile (m)
$M_s(t)$	shaking moment exerted by CBCP on mechanism frame (N m)

1. Introduction

A steady drive speed is often desired for rotating machinery, in order to decrease vibration and noise levels, extend fatigue life, reduce wear, ensure precise operation, etc. However, high-speed industrial machinery often exhibits substantial drive speed fluctuations due to the high torques required to accelerate and decelerate the mechanism inertias. Similar problems are encountered in

combustion engines in which the combination of inertial forces (due to the slider-crank mechanisms) and gas forces causes the crankshaft speed to fluctuate. Mounting a flywheel or adding a friction damper are simple and classical solutions for reducing drive speed fluctuations. However, a large flywheel compromises the start/stop behavior of industrial machinery, as well as the responsiveness of, e.g. a car's combustion engine, whereas a friction damper leads to an increased energy consumption.

A more intelligent solution is *input torque balancing* (ITB). The purpose of ITB is to substantially reduce or eliminate the *input torque*, that is, the torque required to drive the mechanism with a constant drive speed. In case the input torque is completely eliminated (e.g. by adding a torque balancing mechanism to the drive shaft), the drive speed is perfectly constant as the net torque acting on the drive shaft is zero. Section 1.1 surveys the state-of-the-art of ITB in mechanism (cam–follower mechanisms and linkages) literature.

Although ITB is a term from mechanism literature, input torque balancing mechanisms have also been proposed in torsional vibration literature. In this context, torque balancing mechanisms are called *dynamic vibration absorbers*, an overview of which is given in Section 1.2. Special attention is given to the *centrifugal pendulum vibration absorber* (CPVA), as the torque balancing mechanism proposed here, the *cam-based centrifugal pendulum* (CBCP) is a variant of it. Section 1.3 introduces the CBCP, whereas Section 1.4 delimits possible application areas for both the CPVA and the CBCP.

1.1. Input torque balancing in mechanism literature

Input torque balancing can be done by adding springs, mass or a combination of both. It is well known in mechanism literature that spring addition has ITB properties that are optimal for a *single* mean drive speed $\omega = 2\pi/T$ (rad/s) only, where T (s) represents the period of motion. On the contrary, mass addition has ITB properties that are optimal for *any* mean drive speed ω, provided that the original[1] mechanism is purely inertial. A mechanism is considered to be purely inertial if it is a kinematic chain of rigid bodies in which only inertial forces and/or other forces proportional to ω^2 are active.

Mass addition can be done in two ways: either by adding mass to the original mechanism's links or by adding extra links. Adding mass to the existing links is mainly applied to (four-bar) linkages, often in combination with force or shaking moment balancing, and generally succeeds at reducing instead of eliminating the input torque. A survey of these methods is given in Ref. [1] and updated in Ref. [2].

Adding extra links (that is, a compensating mechanism) applies to both linkages and cam–follower systems. Compensating mechanisms providing complete ITB are often based on cams. The simplest cam-based mechanism is an ordinary cam–follower mechanism, where either the follower inertia or a spring working against the follower acts as an accumulator of energy [3–6]. The main disadvantage of using the follower kinetic energy is that the resulting cam

[1]Throughout this paper, the term *original* mechanism will denote the mechanism to be input torque balanced. Furthermore, the input torque balancing mechanism will be termed the *compensating* mechanism, whereas the *combined system* is the ensemble of the original and the compensating mechanism.

displacement is generally not periodical, such that not an ordinary disc cam, but an expensive indexing cam must be used. As already mentioned, the main disadvantage of using the spring potential energy is that the ITB properties are optimal for a single ω only. The CBCP proposed here combines the best of both worlds: it can completely torque balance a purely inertial mechanism for any speed, using an ordinary disc cam.

Other, more complicated cam mechanisms have been suggested. Tidwell et al. [7] suggest that a linear spring could be used in conjunction with a wrapping cam (this is a cam wrapped by a belt or chain) to balance the input torque of a crank-rocker four-bar linkage. Funk and Han [8] introduce a mechanism consisting of a gear pair, a closed-track cam and a rotating member. Teng et al. [9] propose a five-bar mechanism with a cam.

Complete ITB is also achieved by mounting a flywheel driven through a noncircular gear pair [2,10]. A survey of various either fluid-based or mechanical flywheels with variable moment of inertia, possibly providing complete ITB, is given in Ref. [11].

1.2. Input torque balancing in torsional vibration literature

The torque balancing devices proposed in torsional vibration literature are all rotary variants of the translational undamped dynamic vibration absorber (TUVA). They are able to cancel out purely harmonic torques. In general, the frequency of these harmonic torques is considered to be an integer multiple $n\omega$ of the average drive speed ω. n is referred to as the *order* of the disturbing torque.

For a torsional system, Den Hartog [12] suggested two types of undamped dynamic vibration absorbers. The *torsional pendulum vibration absorber* (TPVA), conceptually shown in Fig. 1(a), takes the shape of a flywheel J_c (kg m^2) attached to the original flywheel J_f through a spring k_c (N m/rad). The TPVA is tuned for a single ω, that is, the speed for which the frequency $n\omega$ of the disturbing harmonic torque coincides with the natural frequency $\sqrt{k_c/J_c}$ of the attached absorber.

This shortcoming is overcome by the *centrifugal pendulum vibration absorber*[2] (CPVA), conceptually shown in Fig. 1(b). The rotor of length L_r (m) revolves around the ground point o_1, and is connected to the coupler (pendulum) c of length L_c (m) by a revolute joint. It is easily shown (see e.g. Ref. [12]), based on the *linearized* equations of motion, that the frequency of the pendulum in the centrifugal field equals $\omega\sqrt{L_r/L_c}$. For any ω, this frequency coincides with the frequency $n\omega$ of the disturbing torque provided that

$$n = \sqrt{\frac{L_r}{L_c}}. \tag{1}$$

If Eq. (1) is satisfied, a CPVA is a torsional undamped dynamic vibration absorber that is tuned correctly for all ω. In that case, the rotor has no oscillatory motion (that is, it rotates at a steady speed ω), while the coupler (pendulum) has a finite oscillatory amplitude.

[2]The CPVA seems to have been invented [13] as early as 1929 (British patent [14] by B.C. Carter). For a thorough account of the history of the CPVA and examples of its practical implementation, the reader is referred to the treatise by Ker Wilson [15].

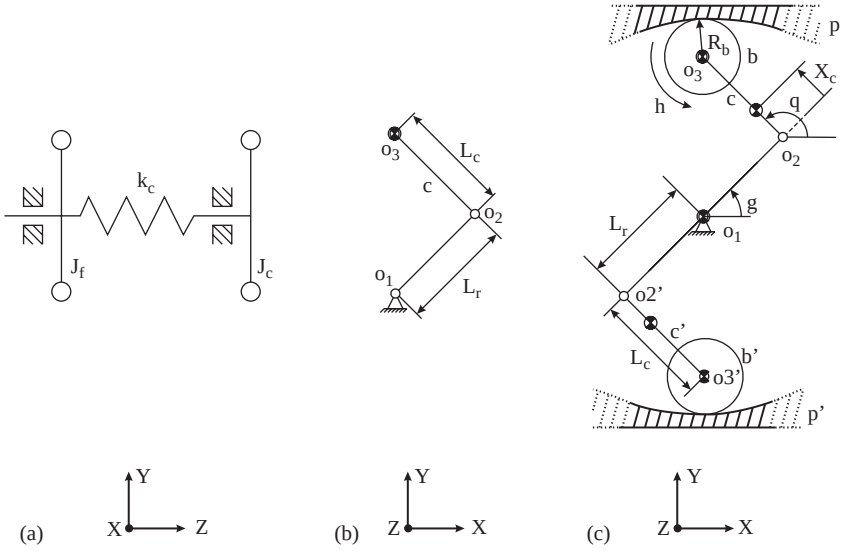

Fig. 1. (a) The torsional pendulum vibration absorber (TPVA), (b) the centrifugal pendulum vibration absorber (CPVA) and (c) the cam-based centrifugal pendulum (CBCP). The Z-axis is defined to be parallel to the drive shaft.

The above result is based on the linearized equations of motion of the CPVA, which are valid for small coupler amplitudes only. However, large amplitudes are sometimes unavoidable if, e.g. the CPVAs mass is to be limited. In that case, nonlinear effects come into play, which cause the torque balancing properties of a CPVA to become fundamentally different from the torque balancing properties of a TUVA. Nonlinear effects are also present in TUVAs. However, as opposed to the CPVA, of which the nonlinear range is inherent from its design, nonlinearities are much more device dependent for TUVAs.

As a first difference, a TUVA is effective for a large range of amplitudes of the disturbing harmonic force. On the contrary, CPVAs designed based on the linearized equations of motion, so-called *linear* CPVAs, are effective for low torque amplitudes only. For higher torque levels, nonlinear effects due to large coupler amplitudes cause the CPVA's frequency to shift. This *detuning* may result in destructive failure of the CPVA [16]. A solution for this is to design CPVAs in which the end point mass moves on a noncircular[3] path, such as a kind of epicycloidal path, the *tautochrone*, proposed by Denman [13,17]. The frequency of these so-called *tautochronic* CPVAs is independent of the coupler (and hence torque) amplitude. In this way, the disastrous detuning is completely avoided. Unfortunately, new dynamic problems have shown up, resulting in smaller allowable torque levels than those initially foreshadowed by the tautochronic CPVAs: it has been observed [18,19] that, if CPVAs are divided into a number of identical masses (e.g. due to spatial

[3]For the conceptual simple pendulum construction of Fig. 1(b), the CPVA is essentially a point mass which moves along a circular path relative to the rotor. Most currently employed variants of the CPVA are, however, of the bifilar type (see e.g. Refs. [13,17]). Bifilar arrangements allow imposing arbitrary noncircular paths.

restrictions), they do not always move in unison: bifurcations may occur in which a single absorber moves out of step with its partners and which limit the allowable torque level.

As a second difference, a TUVA is capable of perfectly balancing a purely harmonic force, as opposed to a (linear or tautochronic) CPVA which induces higher torque harmonics, again due to nonlinear effects. It has, however, been shown [20,21] that subharmonic absorber pairs can provide a solution. These tautochronic absorber pairs that are tuned to one-half of the frequency of the disturbing torque are theoretically effective in the fully nonlinear operating range and are capable of perfectly cancelling a purely harmonic torque of frequency $n\omega$. The price to be paid is a double number of absorbers. Furthermore, some questions remain [21], such as the dynamic stability. Recent results concerning these subharmonic absorber pairs can be found in Ref. [22].

CPVAs have mainly been applied in large stationary engines and aircraft engines. They have also been used to control the fuselage shake in helicopters produced by rotor-associated fluctuating aerodynamic forces, see e.g. Ref. [23]. A new impetus to the study of CPVAs was given by the study [17] by Borowski et al. who established the feasibility of crankshaft-mounted CPVAs for reducing crankshaft torsional vibration in four-cylinder automobile engines.

For both the TPVA and the CPVA, active variants have recently been proposed (respectively called the *delayed resonator* and the *centrifugal delayed resonator*), in which a control torque is applied to actively control the torque balancing properties. For an overview of the state-of-the-art of these devices, the reader is referred to Refs. [24,25], respectively.

1.3. The cam-based centrifugal pendulum

The balancing mechanism proposed here is the cam-based centrifugal pendulum of Fig. 1(c). The rotor, with mass m_r (kg), centroidal moment of inertia J_r (kg m^2) and length $2L_r$ (m), revolves around the ground point o_1. Revolute joints connect the couplers c and c', which each have mass m_c (kg), centroidal moment of inertia J_c (kg m^2) and length L_c (m), with the rotor. The rolling bodies b and b', both having a mass m_b (kg), centroidal moment of inertia J_b (kg m^2) and radius R_b (m), are connected to the corresponding couplers by a revolute joint. These revolute joints are implemented as a bearing, of which the inner ring is fixed to the coupler, and of which the outer ring is the rolling body. $g(t)$ (rad) and $q(t)$ (rad), respectively, denote the rotor's and the coupler's rotation angle w.r.t. the X-axis, whereas $h(t)$ is the rotation angle of the rolling body. As opposed to $g(t)$ and $q(t)$, $h(t)$ needs no definition w.r.t. the X-axis because of the axisymmetry of the rolling body b.

Rotation of the rotor generates centrifugal forces that push b and b' against the internal cams p and p', respectively. p and p' are fixed to the mechanism frame and identical but rotated 180° with respect to each other. The rotor is assumed to be symmetrical w.r.t. the point o_1 such that its center of mass coincides with o_1. The coupler c is assumed to be symmetrical w.r.t. the line o_2-o_3. Consequently, its center of mass lies along this line. Because of the axisymmetry of the rolling body b, its center of mass coincides with the point o_3.

Because of its symmetry w.r.t. o_1, the mechanism is completely force balanced. However, the contact forces between the cams and the rolling bodies exert a nonzero shaking moment (along the Z-axis) on the mechanism frame. Furthermore, due to the fact that the cams cannot lie in the

same plane, the contact forces also exert bending moments (along the X- and Y-axis) on the drive shaft. Due to symmetry, the shaking and bending moments are pure couples.

The CBCP combines the CPVA, well-known in torsional vibration literature, with a torque balancing principle well-known in mechanism literature, that is, the use of cams to generate arbitrary torques. To the authors' knowledge, the CBCP has not yet been described in the open literature.

1.4. CPVA or CBCP?

In order to compare the application potential of both the CPVA and the CBCP, a distinction will be made based on the nature of the original system: (i) a (dominantly or purely) *inertial* system is a kinematic chain of rigid bodies in which the (dominating or sole) forces are inertial forces and/or other forces proportional to ω^2; (ii) a *noninertial* system is a system in which the dominating forces are not proportional to ω^2 (e.g. spring forces, aerodynamic forces, etc.); and (iii) a *mixed* system is a system in which inertial and noninertial forces are equally important.

For (dominantly or purely) inertial systems, such as weaving looms or packaging machines, the CBCP outperforms the CPVA as it provides full[4] balancing (whereas the CPVA only provides partial balancing and induces higher torque harmonics) for any ω. Furthermore, the CBCP does not exhibit the dynamic instabilities of the CPVA for it is a kinematically determined mechanism, as shown in Section 2.

For noninertial systems, such as helicopter fuselages excited by rotor-associated aerodynamic forces, the CPVA is the only good choice as it is capable of adjusting its amplitude of motion to match the varying disturbing torque levels. The CBCP is in fact useless as the only forces it is able to compensate for must be proportional to ω^2, which is obviously not the case for, e.g. aerodynamic forces.

In mixed systems, combining the CPVA and the CBCP seems to be the best solution. As the CBCP takes up the inertial part of the disturbing torque, the torque to be compensated for by the CPVA is much smaller than the original torque. Consequently, the oscillation amplitude of the CPVA's coupler can be smaller, so that it is more likely to remain in its linear range of operation, resulting in fewer dynamic problems due to nonlinearities. Examples of these mixed systems are quite prominent, as e.g. all reciprocating engines (internal combustion engines) or machines (compressors) are characterized by a combination of inertial forces and noninertial gas forces.

This paper focusses on applying the CPVA to high-speed cam–follower systems. Dynamic problems due to drive speed fluctuations in these systems have been reported as early as 1962 [4]. Drive speed fluctuations cause the follower motions to be inaccurate, as the cams are designed for constant drive speed. Consequently the follower accelerations exhibit undesired harmonics which may excite machine resonances, causing vibrations, noise, fatigue and wear.

In order to overcome these problems, the authors have previously [26] introduced *inertially compensated* cams, of which the motion law is adapted to the camshaft speed fluctuation. These cams yield accurately realized follower motions, combined with a small flywheel. However,

[4]Full balancing means cancelling out the full input torque, whereas partial balancing means cancelling out one or several input torque *harmonics*.

inertially compensated cams are not always applicable. Such a situation occurs if there exists a variable synchronization between multiple cam–follower systems mounted on the same drive shaft. In that case input torque balancing of the separate cam–follower systems using, e.g. the CBCP seems to be the best solution.

2. Derivation of the describing equation

This section shows how the cams of the CBCP can be calculated. The derivation of the describing equation which governs the cam design is based on the following assumptions: (i) no friction in the revolute joints, (ii) the rolling bodies roll[5] over the internal cams without sliding, (iii) all bodies are rigid and (iv) the rolling bodies are always in contact with the cams. (i) and (ii) imply that there is no energy dissipation in the CBCP, which, in combination with (iii) allows considering the CBCP as purely inertial. (ii) and (iv) allow considering the CBCP as a kinematically determined mechanism with one degree-of-freedom, that is, the drive shaft angle g (see Fig. 1(c)). In Ref. [1] it was shown that for purely inertial, single-degree-of-freedom mechanisms, the input torque M (N m) and the input angular velocity $\dot{g}$ (rad/s) are related to the kinetic energy T (J) by

$$M = \frac{1}{\dot{g}} \frac{\mathrm{d}T}{\mathrm{d}t}, \tag{2}$$

where all variables are functions of time t, and a dot $(\dot{})$ denotes a time derivative. Consequently, M_c (N m), the CBCP's input torque, is given by

$$M_c = \frac{1}{\dot{g}} \frac{\mathrm{d}T_c}{\mathrm{d}t}, \tag{3}$$

where T_c denotes the kinetic energy of the CBCP. The dynamic equation that governs the cam design will now be derived by imposing, $\forall t \in [0, T]$ that,

$$\begin{cases} M_o(t) + M_c(t) = 0, \\ \dot{g}(t) \equiv \dfrac{2\pi}{T}, \end{cases} \tag{4}$$

where $M_o(t)$ (N m) denotes the original mechanism's input torque. Eq. (4) states that the net input torque to impose a perfectly constant input angular velocity $\dot{g}$ to the combined system should be zero. It is assumed that the original system is also a mechanism with one degree-of-freedom (that is, the same drive shaft angle g). However, no assumption is made concerning the nature of $M_o(t)$: for instance, the original mechanism may be noninertial. In that case the CBCP only provides full torque balance if the actual drive speed of the combined system corresponds to the period of motion T considered during the CBCP design.

[5]In fact, friction is necessary to avoid slipping of the rolling bodies. However, as no slipping occurs, these friction forces are not dissipative.

Multiplying Eq. (4) with $\dot{g}(t) \equiv 2\pi/T$, and integrating between 0 and t yields

$$\frac{2\pi}{T}\int_0^t M_o(\tau)\,\mathrm{d}\tau + \frac{2\pi}{T}\int_0^t M_c(\tau)\,\mathrm{d}\tau = 0.$$

Since Eq. (3) shows that

$$T_c(\tau) = \int M_c(\tau)\dot{g}(\tau)\,\mathrm{d}\tau = \int M_c(\tau)\frac{2\pi}{T}\,\mathrm{d}\tau$$

and defining

$$E_o(\tau) = \int M_o(\tau)\dot{g}(\tau)\,\mathrm{d}\tau = \int M_o(\tau)\frac{2\pi}{T}\,\mathrm{d}\tau,$$

the previous equation can be restated as

$$E_o(t) - E_o(0) + T_c(t) - T_c(0) = 0$$

or

$$E_o(t) + T_c(t) = E_o(0) + T_c(0). \tag{5}$$

The energy function $E_o(t)$ (J) can be interpreted as follows. If the original mechanism is not conservative, $E_o(t)$ represents the sum of its kinetic, potential and dissipated energy as a function of time. If the original mechanism is conservative, $E_o(t)$ equals the sum of kinetic and potential energy. If it is purely inertial, $E_o(t)$ is equivalent to the kinetic energy $T_o(t)$.

Eqs. (4) and (5) will now be transformed into differential equations in $q(t)$ by elaborating the expressions for $T_c(t)$ and $M_c(t)$. Based on $q(t)$, the cam profile can be easily determined[6] using classical analytical geometry results.

2.1. Kinetic energy expression

Due to the mechanism symmetry, only[7] the rotor and the bodies c and b need to be considered for determining $T_c(t)$:

$$T_c(t) = \frac{J_r\dot{g}^2}{2} + 2\left(\frac{J_c\dot{q}^2}{2} + \frac{m_c v_{Cc}^2}{2}\right) + 2\left(\frac{J_b\dot{h}^2}{2} + \frac{m_b v_{Cb}^2}{2}\right), \tag{6}$$

where $v_{Cc}(t)$ and $v_{Cb}(t)$ (m/s) denote the absolute velocity of the centers of mass of the coupler and the rolling body, respectively. Kinematic analysis of the mechanism yields

$$v_{Cc}^2 = L_r^2\dot{g}^2 + X_c^2\dot{q}^2 + 2L_rX_c\dot{g}\dot{q}\cos(g-q), \tag{7}$$

$$v_{Cb}^2 = L_r^2\dot{g}^2 + L_c^2\dot{q}^2 + 2L_rL_c\dot{g}\dot{q}\cos(g-q), \tag{8}$$

where X_c determines the location of the center of mass of the coupler along the line $o_2 - o_3$ (see Fig. 1(c)). As the purpose of the CBCP is to keep the camshaft speed constant, $\dot{g}(t)$ equals $2\pi/T$.

[6]This derivation has not been included for reasons of brevity.

[7]The dynamic effects due to the mass and moment of inertia of the intermediate bodies between the inner and the outer bearing ring (such as the balls in a ball bearing) are neglected.

Due to the fourth design assumption, $\dot{h}^2(t)$ equals $v_{Cb}^2(t)/R_b^2$. Based on these observations and Eqs. (7–8), expression (6) is transformed[8] into

$$T_c(t) = \frac{J_1^*(2\pi/T)^2}{2} + \frac{J_2^*\dot{q}^2}{2} + J_3^*\left(\frac{2\pi}{T}\right)\dot{q}\cos\left(\frac{2\pi}{T}t - q\right), \tag{9}$$

where

$$J_1^* = J_r + 2(m_c L_r^2 + m^* L_r^2), \tag{10}$$

$$J_2^* = 2(J_c + m_c X_c^2 + m^* L_c^2), \tag{11}$$

$$J_3^* = 2(m_c X_c L_r + m^* L_c L_r), \tag{12}$$

$$m^* = \frac{J_b}{R_b^2} + m_b. \tag{13}$$

2.2. Input torque expression

Applying Eq. (9) to Eq. (3) and substituting $\dot{g}$ by $2\pi/T$ yields

$$M_c = \frac{1}{2\pi/T} J_2^* \dot{q}\ddot{q} + J_3^* s, \tag{14}$$

where

$$s(t) = \ddot{q}\cos\left(\frac{2\pi}{T}t - q\right) - \dot{q}\sin\left(\frac{2\pi}{T}t - q\right)\left(\frac{2\pi}{T} - \dot{q}\right). \tag{15}$$

2.3. Describing equation

Substituting Eq. (14) into Eq. (4) yields

$$\frac{1}{2\pi/T} J_2^* \dot{q}\ddot{q} + J_3^* s + M_o(t) = 0. \tag{16}$$

Taking into account expression (15) for $s(t)$ reveals that, for given $M_o(t)$, Eq. (16) constitutes a second-order, nonlinear, explicit (ordinary) differential equation (ODE) in $q(t)$. However, this second-order differential equation has only one independent initial condition (that is, $q(0) = q_0$) as it is obtained by taking the time derivative of the following first-order, nonlinear, implicit (ordinary) differential equation:

$$\frac{J_2^*\dot{q}^2}{2} + J_3^*\frac{2\pi}{T}\dot{q}\cos\left(\frac{2\pi}{T}t - q\right) + E_o(t) = \frac{J_2^*\dot{q}_0^2}{2} + J_3^*\frac{2\pi}{T}\dot{q}_0\cos(q_0) + E_{o,0}, \tag{17}$$

where the subscript 0 indicates values at time instant $t = 0$ s of the corresponding time-dependent quantities. This ODE is obtained by substituting into Eq. (5) the expression (9) for $T_c(t)$, replacing

[8] As $\dot{g}(t) \equiv 2\pi/t$, $g(t)$ equals $2\pi/T \cdot t + g(0)$, where $g(0)$ is assumed to be zero. This does not compromise the generality of the equations.

$\dot{g}(t)$ by $2\pi/T$ and eliminating common terms on the left- and the right-hand sides. From an analytical point of view, solving q from either Eq. (16) or Eq. (17) is equivalent. However, from a numerical point of view, it is not, as shown in Section 3.

3. Solution of the describing equation

Despite the simplicity of the mechanism, the cam design is governed by a nonlinear, second-order, explicit differential equation. Using general-purpose ODE solvers, as those included in MATLAB, is cumbersome as these solvers require initial conditions for q and $\dot{q}$. As already explained, $\dot{q}(0)$ cannot be chosen independently from $q(0)$ as Eq. (16) is the time derivative of the first-order ODE (17). This means that a compatibility condition must be established which relates $\dot{q}(0)$ to $q(0)$. In order to avoid this, a different solution strategy has been adopted, that is, choosing a good parameterization for $\dot{q}$ (a finite Fourier series), and then determining the unknown parameters by solving a nonlinear least-squares problem.

3.1. Parameterization of the solution

As the CBCP makes one complete revolution in one period's time, $\dot{q}(t)$ is a periodical function with period T and $q(T) - q(0) = 2\pi.\dot{q}(t)$ can therefore be parameterized as a Fourier series with period T and average value $2\pi/T$:

$$\dot{q}(t) = \frac{2\pi}{T} + \sum_{k=1}^{\infty} a_k \cos(k\omega t) + b_k \sin(k\omega t),$$

where $\omega = 2\pi/T$. Solving Eq. (16) is now equivalent to determining the unknown amplitudes a_k and b_k, $k = 1 \ldots \infty$. In order to limit the number of unknown parameters, the Fourier series is truncated after K harmonics

$$\hat{\dot{q}}(t) = \frac{2\pi}{T} + \sum_{k=1}^{K} a_k \cos(k\omega t) + b_k \sin(k\omega t), \tag{18}$$

and hence

$$\hat{q}(t) = C + \frac{2\pi t}{T} + \sum_{k=1}^{K} \frac{1}{k\omega}(a_k \sin(k\omega t) - b_k \cos(k\omega t)), \tag{19}$$

$$\hat{\ddot{q}}(t) = \sum_{k=1}^{K} k\omega(-a_k \sin(k\omega t) + b_k \cos(k\omega t)). \tag{20}$$

The hats ($\hat{}$) are introduced since, due to the truncation of the Fourier series, not the exact solution q is calculated but an approximation $\hat{q}$ of it. This approximation will be different if it is obtained based on Eq. (16) or Eq. (17). Therefore, these two approximations will be denoted as $\hat{q}_1$ and $\hat{q}_2$, respectively.

Obviously, the value of K is a compromise between obtaining an accurate solution and limiting the number ($2K$) of unknown parameters. It has been found for the design example outlined hereafter that $K = 20$ is a reasonable choice. The $2K$ unknown parameters are grouped into the parameter vector $\mathbf{z} \in \mathscr{R}^{2K}$:

$$\mathbf{z} = [a_1 \; b_1 \; \ldots \; a_K \; b_K].$$

The integration constant C is not part of $\mathbf{z}$ since its value is determined by the initial condition $\hat{q}(0) = q_0$. Because of the parameterization, $\hat{q}$ and its derivatives are denoted as $\hat{q}(t, \mathbf{z}), \dot{\hat{q}}(t, \mathbf{z})$ and $\ddot{\hat{q}}(t, \mathbf{z})$.

3.2. Nonlinear least-squares problem

The determination of the unknown parameter vector $\mathbf{z}$ is done by solving a nonlinear least-squares problem. To this end, the torque residual function $r_1(t)$ is defined, based on Eq. (16), as

$$r_1(t, \mathbf{z}) = M_c + M_o = \frac{1}{2\pi/T} J_2^* \dot{\hat{q}} \ddot{\hat{q}} + J_3^* s + M_o. \tag{21}$$

Due to the parameterization as a finite Fourier series, $\hat{q}$ and its derivatives depend on $\mathbf{z}$. Hence also r_1 depends on $\mathbf{z}$ and is therefore denoted as $r_1(t, \mathbf{z})$. The unknown parameter vector $\hat{\mathbf{z}}_1$ (and hence the approximate solution $\hat{q}_1$ of the ODE) are now determined based on the following unconstrained optimization problem:

$$\hat{\mathbf{z}}_1 = \min_{\mathbf{z} \in \mathscr{R}^{2K}} \int_0^T r_1^2(t, \mathbf{z}) \, \mathrm{d}t. \tag{22}$$

This is a nonlinear least-squares problem. In order to numerically solve this problem, it is approximated by

$$\hat{\mathbf{z}}_1 = \min_{\mathbf{z} \in \mathscr{R}^{2K}} T_s \sum_{k=1}^{N} r_1^2((k-1)T_s, \mathbf{z}), \tag{23}$$

where $f_s = 1/T_s$ is the rate at which $r_1(t, \mathbf{z})$ is sampled, and $N = T/T_s$ denotes the number of sampling points within one period of motion. Although this problem can be solved using a general-purpose unconstrained optimization technique, it is better to apply a dedicated nonlinear least-squares technique such as the Levenberg–Marquardt algorithm which exploits the special structure of the gradient and Hessian matrix, and hence results in faster convergence. This algorithm is implemented in the `lsqnonlin` algorithm of the MATLAB OPTIMIZATION TOOLBOX which has been used to solve Eq. (23). Once $\hat{\mathbf{z}}_1$ is calculated, $\hat{q}_1$ and its time derivatives can be determined based on Eqs. (18)–(20).

Determination of $\hat{q}_2$ can be done by proceeding in a similar way, using an energy residual $r_2(t, \mathbf{z})$, defined based on Eq. (17). Because of the analytical equivalence of Eqs. (16) and (17), it can be intuitively understood that $\hat{q}_2 \approx \hat{q}_1$. However, as $\hat{q}_1$ is the minimizer of

$$T_s \sum_{k=1}^{N} r_1^2((k-1)T_s, \mathbf{z})$$

it is obvious that

$$\sum_{k=1}^{N} r_1^2((k-1)T_s, \hat{\mathbf{z}}_1) \leqslant \sum_{k=1}^{N} r_1^2((k-1)T_s, \hat{\mathbf{z}}_2). \tag{24}$$

In other words, the rms value of the torque residual $r_1(t, \mathbf{z}) = M_c(t) + M_o(t)$ is smaller for $\hat{q}_1$ than for $\hat{q}_2$. Hence, $\hat{q}_1$ should be preferred over $\hat{q}_2$ for the compensating mechanism's ultimate goal is to provide the smallest possible torque residual.

4. Design example

In this section, the theory developed in the previous sections is applied to design a CBCP for a high-speed cam–follower system. First the cam–follower system to be balanced is introduced. Second, the optimization of the design parameters is discussed. Third, the design results are presented.

4.1. Problem definition

The cam–follower system to be balanced is assumed to be purely inertial. Although this assumption may seem quite restrictive, purely inertial systems quite effectively represent high-speed cam–follower systems [1]. The absence of springs, imposed by this prerequisite, implies that the contact between the cam and the follower must be ensured by using a conjugate cam pair, as shown in Fig. 2. Because the cam–follower system is purely inertial, $E_o(t) \equiv T_o(t)$, where $T_o(t)$, the fluctuating part of the kinetic energy of the cam–follower system, is given by

$$T_o(t) = \frac{J\dot{f}^2}{2}. \tag{25}$$

$\dot{f}(t)$ denotes the velocity of the follower and J (kg m^2) the follower's inertia w.r.t. its center of rotation (point o_5 in Fig. 2). The mechanism's period of motion is $T = 0.0667$ s, which corresponds to an average drive speed ω of 900 rpm. Its oscillating, statically balanced follower has a centroidal moment of inertia J of 0.2633 kg m^2 and constitutes the sley of an industrial weaving loom. Fig. 3 shows its desired motion $f(t)$, which is synthesized as a finite Fourier series with six harmonics.

As the cam–follower system is a single-degree-of-freedom mechanism assumed to be purely inertial, Eq. (2) applies, and the input torque $M_o(t)$ (N m) is given by

$$M_o = \frac{1}{2\pi/T} J\dot{f}\ddot{f}. \tag{26}$$

It was chosen to input torque balance this mechanism using two identical CBCPs for this will result in smaller cams since each CBCP has to deliver half of the required torque. Secondly, using two CBCPs allows mutual cancellation of their bending moments exerted on the drive shaft.

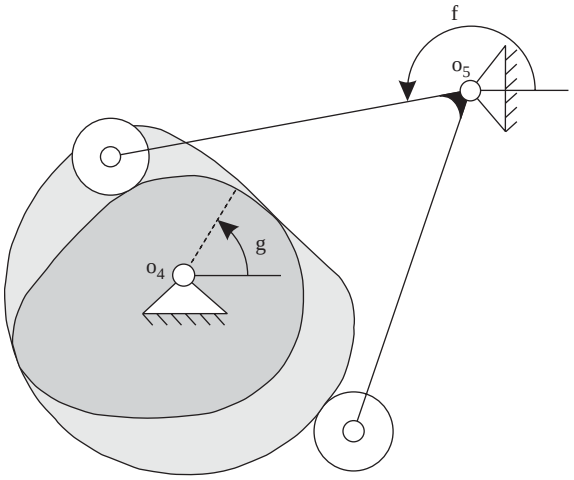

Fig. 2. Conjugate cam–follower system.

4.2. Design optimization

An inspection of the describing equation (16) shows that, given the torque $M_o(t)$ to be balanced and the period of motion T, q depends on three *fundamental* parameters: J_2^*, J_3^* and the initial condition q_0. Since Eqs. (11)–(13) show J_2^* and J_3^* to depend on $L_c, L_r, R_b, m_c, m_b, J_c, J_b$ and X_c, the following nine *design* parameters affect q and hence the shape and the technological properties of the CBCP: the kinematic parameters L_c, L_r and R_b, the mass parameters m_c, m_b, J_c, J_b and X_c and the initial condition q_0. These parameters can be determined based on an optimization problem so as to obtain a compact and technologically feasible mechanism.

Several criteria can be chosen for the optimization: minimal size of the cams, maximal bearing lifetime, etc. The goal function chosen here is minimal equivalent inertia J_{eq} (kg m^2). Assuming that the original system is conservative, the combined system has constant energy such that it can be considered as an equivalent flywheel with inertia J_{eq}, turning at $2\pi/T$ (rad/s). The numerical value of J_{eq} is determined by equating the kinetic energy of the equivalent flywheel and the constant energy of the combined system

$$\frac{J_{\text{eq}}(2\pi/T)^2}{2} = E_o(t) + T_c(t) = E_{o,0} + T_{c,0}. \tag{27}$$

It can be shown that J_{eq} is independent of T, provided that the original mechanism is purely inertial ($E_o(t) \equiv T_o(t)$). The rationale for choosing J_{eq} as the optimization criterion is that inertia minimization was exactly the reason for using a torque balancing mechanism instead of a large flywheel.

The optimization constraints are concerned with the technological feasibility of the mechanism, as well as the avoidance of collisions between the moving parts. Fig. 4 shows the assembly of the rotor r, coupler c and rolling body b. When the coupler moves w.r.t. the rotor, two collisions may

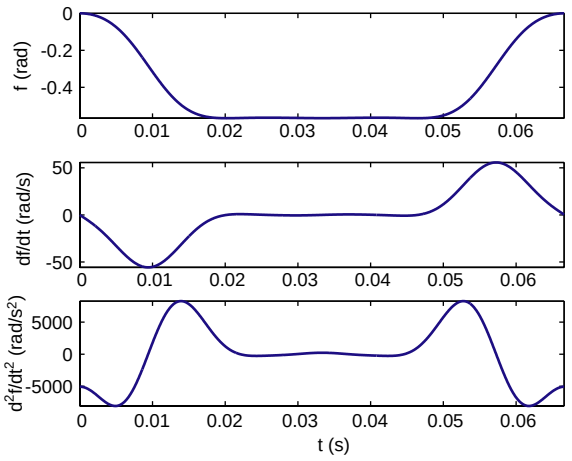

Fig. 3. Desired position, velocity and acceleration of the design example's cam follower.

occur: (i) a collision between the outer bearing ring (that is, the rolling body b) and the cylinder of radius R_{r1} that belongs to the rotor and (ii) a collision between the coupler and this same cylinder.

The technological constraints are the following. Firstly, there must always be contact between the rolling bodies and the cams. This can be mathematically expressed by imposing that the contact force $N_c(g)$ (N) between the cams and the rolling bodies should have a minimum $N_{c,\min}$ over $[0, 2\pi]$ which is greater than zero, or for robustness reasons, greater than some positive lower bound $N_c^{\mathrm{m}} = 100\,\mathrm{N}$. Secondly, the Hertzian pressure $\sigma_H(g)$ (MPa) in the cam should have a maximum $\sigma_{H,\max}$ over $[0, 2\pi]$ which is less than some upper bound $\sigma_H^M = 900\,\mathrm{MPa}$. Thirdly, the lifetime L_b (h) of the bearing that implements the revolute joint between the rolling body and the coupler, and the lifetime L_c (h) of the bearing that implements the revolute joint between the rotor and the coupler should be greater than 50,000 h (at 900 rpm).

In order to mathematically translate the aforementioned technological and collision constraints, the design parameters are replaced by a number of optimization variables through parameterization of the rotor's and coupler's shape. As this requires a lengthy discussion, a full presentation of the design optimization is deferred to the companion paper [27].

4.3. Design results

Table 1 gives the numerical values of the design parameters resulting from the design optimization discussed in the companion paper [27]. These values in turn determine the numerical values of J_2^* and J_3^* through Eqs. (11–13). Fig. 5 shows $\hat{q}_1(t)$ and its derivatives, as calculated by the `lsqnonlin` algorithm, with $K = 20$. Fig. 6 shows the CBCP with the rotor and the couplers in their positions at time instant $t = 0\,\mathrm{s}$. The minimum and maximum of the cam radius $r(g)$ over $[0, 2\pi]$ are: $r_{\min} = 146.1\,\mathrm{mm}$ and $r_{\max} = 154.8\,\mathrm{mm}$. Thus, the stroke of the mechanism is 8.7 mm. The limited value of $r_{\max}$ illustrates that the resulting mechanism is quite compact.

An interesting check of the solution is the torque residual $r_1 = M_o + M_c$. Due to the truncation of the Fourier series when solving the differential equation, the torque residual is not perfectly zero. Fig. 7(a) shows M_c and M_o, whereas Fig. 7(b) shows the torque residual, which is negligible w.r.t. the maximal value of M_o, equal to 880 N m. Furthermore, a dominant 21st harmonic is clearly present, originating from the fact that $K = 20$ harmonics are used for solving Eq. (16).

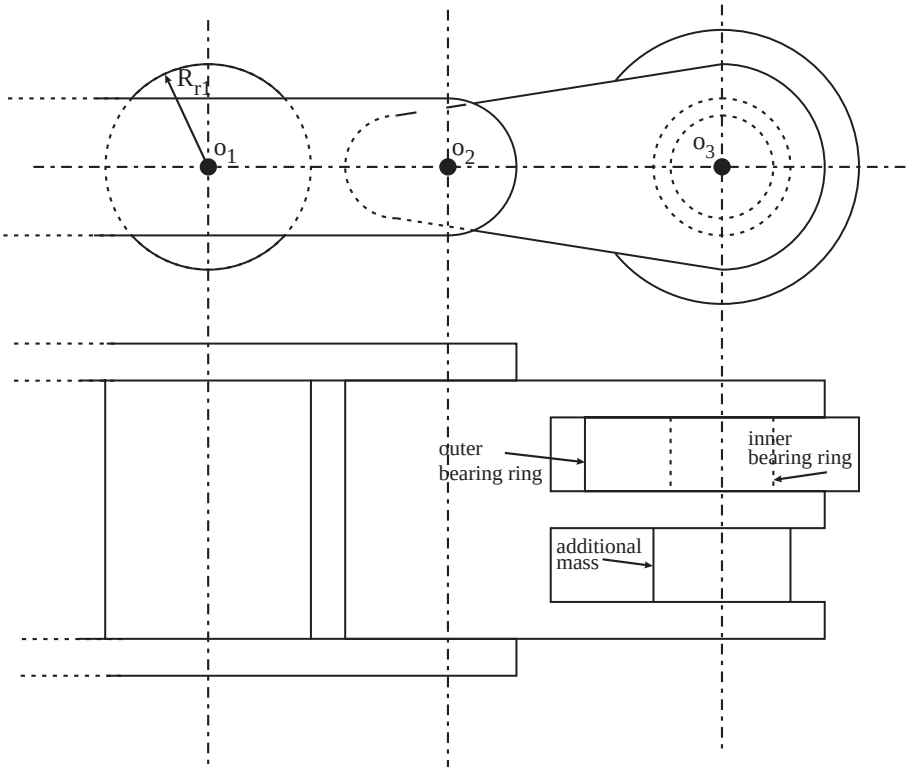

Fig. 4. Front and top view of the assembled rotor, coupler and rolling body.

Table 1
Design example: numerical values of the design parameters

L_r (m)	L_c (m)	R_b (m)
0.0720	0.0831	0.050
m_c (kg)	X_c (m)	m_b (kg)
14.473	0.0437	1.841
J_c (kg m^2)	J_b (kg m^2)	q_0 (°)
0.03239	0.002568	100.16

The value of the goal function for this design is $J_{\text{eq}} = 0.4060\,\text{kg m}^2$. In order to asses this value, the original mechanism's equivalent inertia $J_{\text{eq},o}$ (kg m^2) is introduced in a similar way as J_{eq}:

$$\frac{J_{\text{eq},o}(2\pi/T)^2}{2} = T_o. \tag{28}$$

As T_o is a function of time, so is $J_{\text{eq},o}$. Since $T_c(t) \geqslant 0$, $\forall t$, the physical lower limit for $T(t) = T_o(t) + T_c(t)$ equals the maximal value of $T_o(t)$. Consequently, the physical lower limit for J_{eq} corresponds to the maximum of $J_{\text{eq},o}(t)$ over $[0, T]$, equal to $0.0919\,\text{kg m}^2$. Hence, J_{eq} is three times greater than its physical lower limit, which is due to the fact that the mechanism must comply with the constraints. Any lower value of J_{eq} would result in a mechanism which does not comply with one of the aforementioned constraints.

For this design, the technological constraints are fulfilled as $N_{c,\min} = 100\,\text{N}$, $\sigma_{H,\max} = 900\,\text{MPa}$, $L_b = 742{,}000\,\text{h}$ and $L_c = 614{,}000\,\text{h}$. Furthermore, no collisions occur between the moving parts.

A final check of the solution is the maximum $M_{s,\max}$ over $[0, T]$ of the shaking moment $M_s(t)$ (N m). For the optimized design, $M_{s,\max}$ equals 211 N m. Whether or not this is an improvement w.r.t. the shaking moment in the original mechanism depends on the way the original mechanism is driven. Two cases are distinguished: (A) an advanced control system is present to impose a steady drive speed and (B) a simple control system is present to keep up the average drive speed, in combination with a flywheel to reduce the drive speed fluctuation. The motor exerts a shaking moment on the mechanism frame, due to the fact that the reaction torque of the motor torque acts on the stator, attached to the mechanism frame. In case A, the motor torque approximately equals M_o, whereas in case B, the motor torque is small. Hence, in the original system, either a shaking moment of 880 N m (case A), or a negligible shaking moment (case B) is present. In the balanced system, the motor torque is zero, for both cases. The shaking moment then originates (if the shaking moment due to the original mechanism is neglected) from the CBCP. Consequently, in

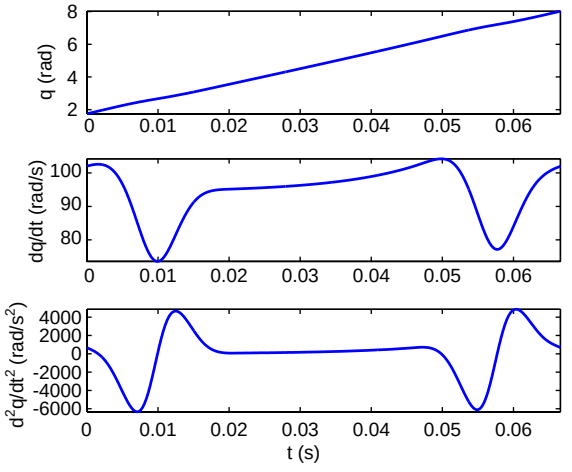

Fig. 5. $\hat{q}_1$ and its first two derivatives for the design example.

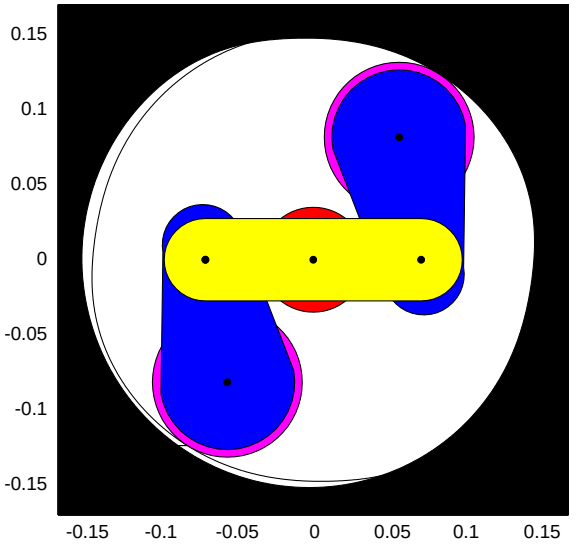

Fig. 6. CBCP resulting from the design optimization. Both the X- and the Y-axis are expressed in (m). The solid boundary indicates the cam against which the upper rolling body rolls. The thin boundary, shown in the left part, and hidden behind the solid boundary in the right part, indicates the cam against which the lower rolling body rolls.

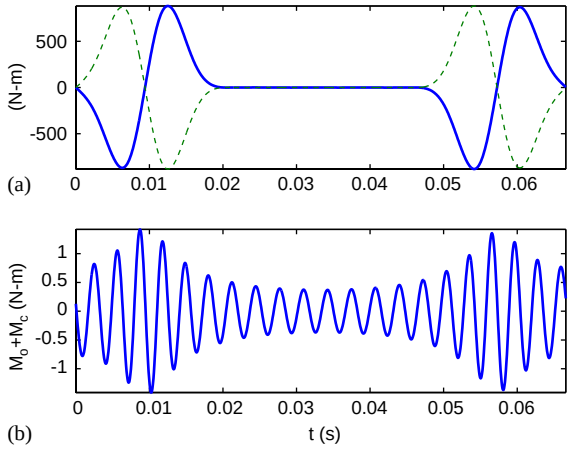

Fig. 7. (a) $M_o(t)$ (dashed line) and $M_c(t)$ (full line) and (b) torque residual for the design example.

case A, a shaking moment of 880 N m is replaced by a shaking moment of 211 N m, whereas in case B, a negligible shaking moment is replaced by a shaking moment of 211 N m.

5. Conclusions

A mechanism, the CBCP, and a design procedure for it have been presented that result in quasi-perfect torque balancing for any drive speed, provided that the original mechanism is purely

inertial. With respect to other mechanisms known in mechanism literature, the CBCP has the advantage of simplicity. Furthermore, the application areas of the CBCP and the CPVA, the ITB mechanism most widely used in torsional vibration literature, have been delimited.

For given design parameters, the cam design is governed by a nonlinear, second-order, explicit differential equation that is the derivative of a nonlinear, first-order, implicit differential equation, and hence has only one independent initial condition. As this introduces a cumbersome compatibility condition, not a conventional ODE solver, but a parameterization as a finite Fourier series and a nonlinear least-squares algorithm have been used to solve the differential equation.

Nine design parameters have been identified, which are determined by means of an optimization problem. The purpose of the optimization problem is to minimize the combined system's equivalent inertia taking into account collision and technological constraints. Application of the CBCP to torque balance a high-speed, purely inertial cam–follower mechanism showed that the optimization results in a compact and technologically feasible mechanism.

Future work will mainly focus on building a CBCP prototype in order to experimentally validate its promising features.

Acknowledgements

Bram Demeulenaere is a Postdoctoral Fellow of the Fund for Scientific Research-Flanders (Belgium) (F.W.O.). This work also benefited from the Belgian Inter-Universitary Poles of Attraction Programme IUAP V/AMS, initiated by the Belgian State, Prime Minister's Office, Science Policy Programming, and K. U. Leuven's Concerted Research Action GOA/99/04. The scientific responsibility is assumed by its authors.

References

[1] R. Berkof, The input torque in linkages, *Mechanism and Machine Theory* 14 (1979) 61–73.
[2] I. Kochev, General method for active balancing of combined shaking moment and torque fluctuations in planar linkages, *Mechanism and Machine Theory* 25 (6) (1990) 679–687.
[3] I. Artobolewski, Das dynamische Laufkriterium bei Getrieben, *Maschinenbautechnik* 7 (12) (1958) 663–667.
[4] E. Sarring, Torque compensation for cam systems, *Transactions of the Seventh Conference on Mechanisms*, 1962, pp. 179–185
[5] C. Benedict, G. Matthew, D. Tesar, Torque balancing of machines by sub-unit cam systems, *Second Applied Mechanism Conference*, 1971, Paper No. 15
[6] M. Nishioka, State of the art of torque compensation cam mechanisms, *Proceedings of the Ninth World Congress on the Theory of Machine and Mechanisms*, 1995, pp. 713–717
[7] P. Tidwell, N. Bandukwala, S. Dhande, C. Reinholtz, G. Webb, Synthesis of wrapping cams, *Journal of Mechanical Design* 116 (1994) 634–638.
[8] W. Funk, J. Han, On the complete balancing of the inertia-caused input torque for plane mechanisms, *Proceedings of the ASME 1996 Design Engineering Technical Conferences and Computers in Engineering Conference*, Paper No. 96-DETC/MECH-1570, 1996
[9] G. Teng, H. Fu, W. Zhou, A new method of torque compensation for high speed indexing cam mechanism, *Journal of Mechanical Design* 121 (1999) 319–323.

[10] D.B. Dooner, Use of noncircular gears to reduce torque and speed fluctuations in rotating shafts, *Journal of Mechanical Design* 119 (1997) 299–306.
[11] D. Ullman, H. Velkoff, An introduction to the variable inertia flywheel (vif), *Journal of Applied Mechanics* 46 (1979) 186–190.
[12] J. Den Hartog, *Mechanical Vibrations*, fourth ed., McGraw-Hill, New York, 1956.
[13] H. Denman, Tautochronic bifilar pendulum torsion absorbers for reciprocating engines, *Journal of Sound and Vibration* 159 (2) (1992) 251–277.
[14] B. Carter, Rotating pendulum absorbers with partly solid and partly liquid inertia members with mechanical or fluid damping, British Patent No. 337,466, 1929.
[15] W. Ker Wilson, *Practical Solution of Torsional Vibration Problems*, third ed., vol. IV, *Devices for Controlling Vibration*, Chapman & Hall, London, 1968
[16] D. Newland, Nonlinear aspects of the performance of centrifugal pendulum vibration absorbers, *Journal of Engineering for Industry* (1964) 257–263
[17] V. Borowski, H. Denman, D. Cronin, S. Shaw, J. Hanisko, L. Brooks, D. Mikulec, W. Crum, M. Anderson, Reducing vibration of reciprocating engines with crankshaft pendulum absorbers, SAE Technical Paper Series, Paper No. 911,876, 1991.
[18] C.-P. Chao, S. Shaw, C.-T. Lee, Stability of the unison response for a rotating system with multiple tautochronic pendulum vibration absorbers, *Journal of Applied Mechanics* 64 (1997) 149–156.
[19] C.-P. Chao, C.-T. Lee, S. Shaw, Non-unison dynamics of multiple centrifugal pendulum vibration absorbers, *Journal of Sound and Vibration* 204 (5) (1997) 769–794.
[20] C.-T. Lee, S. Shaw, On the counteraction of periodic torques for rotating systems using centrifugally driven vibration absorbers, *Journal of Sound and Vibration* 191 (5) (1996) 695–719.
[21] C.-T. Lee, S. Shaw, V. Coppola, A subharmonic vibration absorber for rotating machinery, *Journal of Vibration and Acoustics* 119 (1997) 590–595.
[22] C.-P. Chao, S. Shaw, The dynamic response of multiple pairs of subharmonic torsional vibration absorbers, *Journal of Sound and Vibration* 231 (2) (2000) 411–431.
[23] W. Paul, Vibration damped helicopter rotor, U.S. Patent No. 3,540,809, 1970.
[24] D. Filipovič, N. Olgac, Delayed resonator with speed feedback—design and performance analysis, *Mechatronics* 12 (2002) 393–413.
[25] M. Hosek, H. Elmali, N. Olgac, A tunable torsional vibration absorber: the centrifugal delayed resonator, *Journal of Sound and Vibration* 205 (2) (1997) 151–165.
[26] B. Demeulenaere, J. De Schutter, Synthesis of inertially compensated variable-speed cams, *Journal of Mechanical Design* 125 (2003) 593–601.
[27] B. Demeulenaere, P. Spaepen, J. De Schutter, Input torque balancing using a cam-based centrifugal pendulum: design optimization and robustness, *Journal of Sound and Vibration* 283 (1 + 2) (2005) 21–46, this issue; doi:10.1016/j.jsv.2004.04.003.